

Computation film cooling from three different holes geometries

A. Khorsi*, A. Azzi**

*University of Sciences and Technologie BP 1505 El Mnaouer, Oran-Algeria, E-mail:azzeddine_khorsi@yahoo.fr

**University of Sciences and Technologie BP 1505 El Mnaouer, Oran-Algeria, E-mail:abbesazzi@yahoo.fr

Nomenclature

D - film cooling hole diameter, mm; s - width of the console and passage, mm; U - velocity, $m.s^{-1}$; δ - boundary layer thickness, mm; Tu - turbulence intensity, %; M - blowing ratio; I - momentum ratio; η - effectiveness.

Subscripts : c - coolant conditions; ∞ - streamwise conditions ; $Plenum$ - plenum conditions.

1. Introduction

The gas turbine engine is one of the most important inventions in the field of man-made power machines because it provides as much as 1500 kW power output. Engineers who design advanced gas turbine engines seek to increase the ratio of the thrust force to the weight and reduce the fuel consumption. The turbine blades must be functional in severe working environments. The pressure of approximately 30 atm and the temperature exceeds 1680°C. Protection of the blades from burn out when they are in direct contact with the hot gas that streaks from the upstream combustor, must be seriously considered.

It is well known that high performance and long life of gas turbine engines are strongly related to the cooling system adopted and its performance. Film cooling is by far the most sophisticated applied technique available and consequently used for high temperature gas turbine systems. From a hydrodynamic point of view, it is well argued that the flow structure in the vicinity of the film cooling discharge holes is extremely complex and leads to several vortex structures.

Analysis of the discrete-film-cooling performance requires the understanding of fundamental jet-in-cross-flow. The jet in cross flow problem has been investigated for over fifty years, and has been discussed by Goldstein and Margason [1]. Numerous parameters affect the cooling performance, such as blowing ratio, density ratio of the coolant and the hot mainstream, free-stream turbulence level, pressure gradient, the curvature, the cooling holes geometry, the holes spacing and row arrangement.

Earlier, Bergles et al. [2] and then Andreopoulos and Rodi [3] studied in details a single perpendicular jet in cross flow and highlighted the importance of jet deflection toward the wall which is associated by lower pressure in the wake and higher pressure in the front of the jet. Low pressure region in the wake is responsible for the flow motion toward the center plane, which promotes the formation of two counter rotating vortexes. Additional vortex structures are detected such as horseshoe vortex, windward and lee vortex. One possibility to enhance the film cooling effectiveness is to destroy the two contra rotating vortexes or at least decrease their intensity. On 2002, Sargison et al.[4] presented a new geometry which is in the middle between a discrete cylindrical hole and spanwise continuous slot.

The work was done in an experimental way for both a flat plate and a profile blade configuration. Later, Azzi & Jubran [5] presented a numerical investigation of geometry similar to that presented by Sargison et al. [4] but with different dimensions as the experimental one was not disposable at that time. In this paper, detailed numerical investigation of the exact geometry and conditions used by Sargison et al. is done using the well stabilized CFX code.

2. Turbulence model

The simulations were processed using the CFX 10.0 software from ANSYS, Inc. In the solver package, the solution of the Reynolds Averaged Navier-Stokes Equations is obtained by using finite volume method with a body-fitted structured grid. A cell-centered layout is employed in which the pressure, turbulence and velocity unknowns share the same location. The momentum and continuity equations are coupled through a pressure correction scheme and several implicit first and second order accurate schemes are implemented for the space and time discretizations. In the present computation, convection terms written in convective form are discretized with a third order upwind-biased scheme.

The turbulence closure is done with the help of the $k - \omega$ shear stress transport (SST) turbulence model of Menter [6]. The main advantage of this model is its capability to be applied in the high Reynolds number region as well as in the near wall regions. The strategy is based on a blend of the $k - \omega$ model of Wilcox [7] in the near wall region and the standard $k - \varepsilon$ model [8] further away from the wall. Due to the high capability behavior of the $k - \omega$ model near the wall, the SST model does not need explicit damping when approaching the wall. The well known dependence of free stream values of ω are eliminated by the blend of the $k - \varepsilon$ model. The details of Reynolds Averaged Navier Stokes equations as well as the SST turbulence model are not given here since they are well documented in the literature.

3. Test case description

Three geometrical configurations which have been studied experimentally by Sargison et al. [4] are reproduced here. The first configuration is streamwise inclined hole which is largely used and well documented in the literature. The second configuration is a rectangular slot inclined too with the same angle. The third configuration is that proposed by Sargison et al. [4] where console stands for converging slot hole. The console is designed to offer an improved cooling and aerodynamic performance of the slot geometry, while retaining the mechanical strength of a row of discrete holes. The cross-section of the console changes from a circular shape at the inlet to a slot

at the exit. In a view side the walls of the console converge, and in plan view the walls diverge, but the convergence is greater than the divergence so that the cross-sectional area decreases and the flow accelerates from inlet to outlet. The minimum hole area is at the throat and hence the maximum flow velocity exists at the hole exit. According to Sargison et al. [4], for such accelerated flow the boundary layer remains laminar, or turbulent boundary layers relaminarize, considerably increasing the efficiency of the console flow compared to shaped holes. The other great advantage of joining the hole exits is that the ejected coolant film is continuous in the span-wise direction (in contrast to cylindrical holes), and the film will not lift off from the blade surface at typical blowing ratios. Consequently, the typical two counter rotating vortices disappear and the film cooling effectiveness increases. The geometry of the console has also been designed to be easily manufactured by available drilling (mechanical or laser) techniques.

4. Geometry and computational domain

The first case presented in Fig. 1, a, is composed of a single row of cylindrical holes inclined by 35° in the stream wise direction. The lateral spacing of the holes is fixed to $3d$. Where d is 20 mm and stands for the hole diameter. The jet length-to-diameter ratio was 5.2. The computational domain extends from the inflow plane to $38d$ in the streamwise direction and from the bottom of the flat plate to $8d$ in the vertical direction. In the spanwise direction, the domain extends from a plane through the middle of the hole to a plane at $1.5d$ in the middle between two injection holes, and symmetry conditions are imposed on these planes. No lateral inclination of the jet, allows the consideration of only half of the flow domain.

The slot computational domain presents a continued rectangular coolant ejection through a rectangular channel inclined by 35° with $20.9 S$ lengths, $S = 5$ mm is the slot width like mentioned in Fig. 1, b. This geometry provides a uniform film protector but with very bad strength resistance for this reason we focused the study on the new converging slot hole geometry.

The console computational domain which is presented in Fig. 1, c has the same dimensions to that described before except that for the spanwise direction which is now fixed at the stands for the diameter of the console inlet and is taken as 25 mm. In order to keep the same equal throat area per unit width for the configurations, the slot width is kept at 5 mm. Finally, for data presentation, the equivalent cylindrical hole diameter of 20 mm is used.

In order to be more precise when applying the inlet boundary conditions, the plenum part was integrated in the computational domain, while the approaching boundary layer was taken to be fully developed. According to Sargison's observations, a seventh power boundary layer according to $U_{inlet} = U_\infty(y/\delta)^{1/7}$ is applied at the main inlet boundary. The main-stream velocity was set to and the boundary layer thickness to $d = \delta$. Uniform distributions of and $k-\varepsilon$, corresponding to a free-stream turbulence intensity of $Tu = 1\%$ were chosen for both the main and plenum inlets boundaries. Automatic wall function, which is a powerful tool in CFX code, is applied by default at all wall boundaries. In this technique, the boundary conditions switch automatically from the high to the low Reynolds

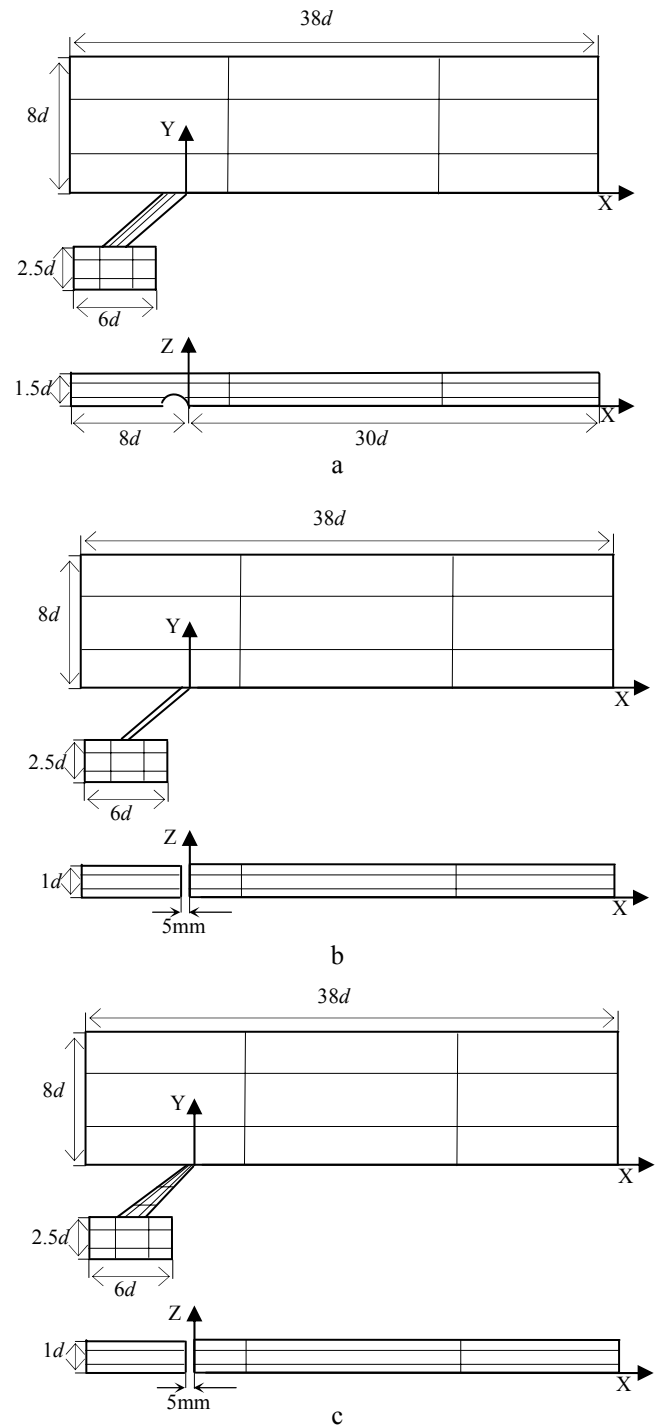


Fig. 1 Computational domain for: a - cylindrical, b - slot, c - console injection

number strategy according to the values at the first node near the wall. Nevertheless, in the present computation, care is taken to be always in the low Reynolds number range. All walls are considered as adiabatic and a difference of 40° between the temperature of the main stream and the plenum is considered.

Preliminary computational tests lead to an optimized grid, composed of nearly half million elements. Due to high convergence of the console, a hybrid computational grid was chosen for the console which is composed of some blocs in structured grids (main and plenum) and an unstructured grid for the console. The grids are highly refined near the walls and use the well known O grid strategy

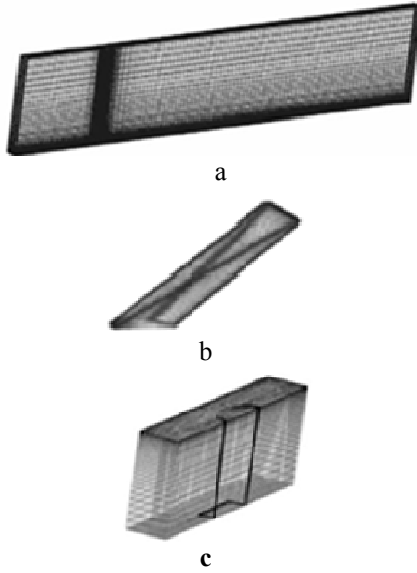


Fig. 2 Hybrid computational grid for the console geometry: a - main flow; b - console; c - plenum

to well describe the vicinity of the hole injection. The quality of the computational grid is highly improved in the sense of aspect ratio and skewness by use of the O grid strategy cited above. Fig. 2 shows the three main parts of the console grid. All the grids are generated by use of the ICEM grid generation tool from ANSYS, Inc.

Table, summarizes the different cases considered in the present study, which match those done by Sargison et al. [4] in their experimental measurements. The plenum injection velocity is computed according to the continuity equation.

Table
Injection conditions for the three geometries

	$I = \rho_c^2 U_c^2 / \rho_\infty^2 U_\infty^2$	$M = \rho_c U_c / \rho_\infty U_\infty$	$U_{Plenum} (m/s)$
Cylinder	0.17	0.4	0.4677
	0.48	0.69	0.7860
	0.67	0.82	0.9285
Slot	0.14	0.37	0.3234
	0.36	0.60	0.7860
	0.75	0.87	0.9285
Console	0.07	0.26	0.2180
	0.30	0.55	0.4613
	0.41	0.64	0.5367

5. Results and discussion

The first validation consists of comparing the so called laterally averaged adiabatic film cooling effectiveness $\langle \eta \rangle$ defined by

$$\langle \eta \rangle = \frac{1}{L} \int_L \eta dz \quad (1)$$

where L represents the spanwise dimension of the flat plate and η is the effectiveness defined by

$$\langle \eta \rangle = \frac{T_\infty - T}{T_\infty - T_c} \quad (2)$$

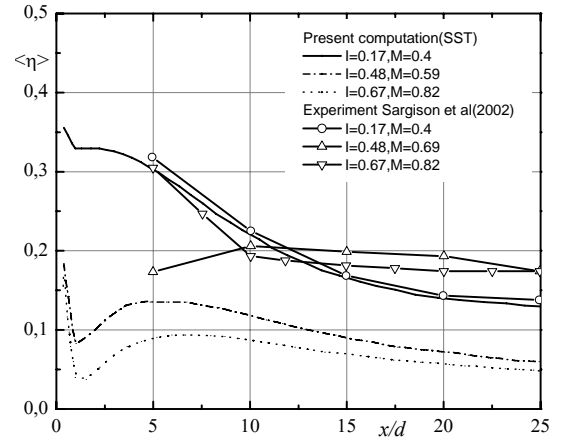


Fig. 3 Longitudinal distribution of $\langle \eta \rangle$ for cylinder

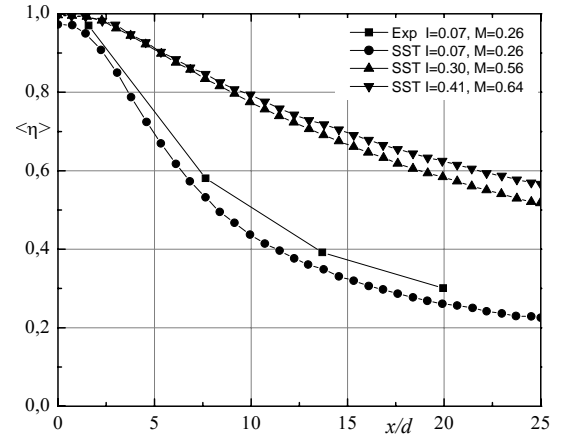


Fig. 4 Longitudinal distribution of $\langle \eta \rangle$ for slot

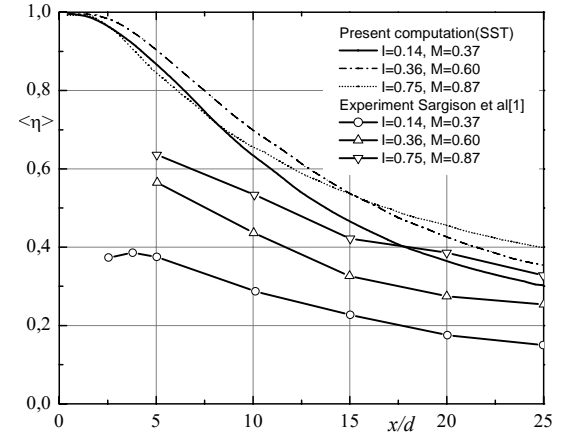


Fig. 5 Longitudinal distribution of $\langle \eta \rangle$ for console

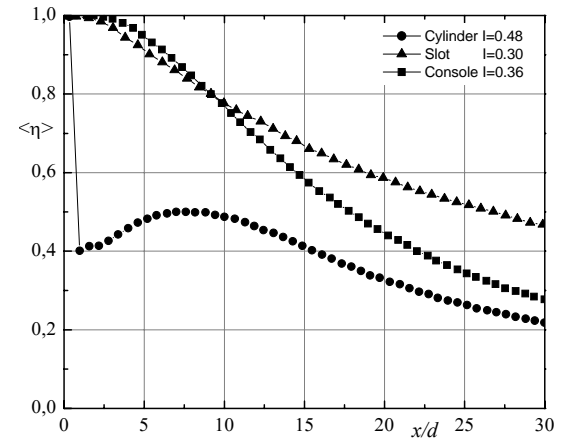


Fig. 6 Centerline effectiveness

Fig. 3 shows the computed longitudinal distributions of $\langle \eta \rangle$ for three blowing ratios in comparison with the experimental measurements of Sargison et al. Fig. 3 is for the cylindrical hole injection while Fig. 4 is for the slot and Fig. 5 is for console geometry.

It can be seen from figure that the computational results agree with the experimental ones only for the lowest blowing ratio in cylindrical injection case. The results show that the laterally averaged effectiveness has its highest value in the vicinity of the injection hole and then it decreases monotonously afterward. When increasing the blowing ratio, the computed results show a rapid decrease immediately downstream of the hole injection and then a net increase until $x/d = 5$. After this position, the cooling effectiveness decrease monotonously. This behavior is common for the two high blowing ratios and is typically indicative that the jet lifts off and reattaches afterward. Surprisingly, the experimental measurement for the highest blowing ratio does not follow this behavior.

As it is expected by previous numerical investigations (with standard $k - \epsilon$ turbulence model), the first order isotropic class of turbulence models (the SST model used here is still in this class) under predict the lateral expansion of the thermal field and consequently under predict the lateral averaged adiabatic film cooling effectiveness, Fig. 3.

Fig. 4 shows the results of the centerline effectiveness obtained for the slot geometry for three blowing ratios. The effectiveness of the lower blowing ratio agrees with that measured by Sargison. The numerical results obtained with the SST model show the typical augmentation of the effectiveness with the increase of the blowing ratio. Fig. 6 shows a comparison of the adiabatic effectiveness between the three holes geometries for the middle blowing ratio. The results show a good cooling with the slot hole, this can be due to the uniformity and the continuity of the coolant injection. The classical cylindrical hole geometry offers the more lower effectiveness comparing with the slot and the new console which presents a medium effectiveness on the other hand, Fig. 5 for the console geometry indicates that the numerical results are now over predicted and follow the same trends as the experimental ones. For both numerical and experimental results, increasing the blowing ratio leads to an improved film cooling effectiveness. This can be explained by the fact that in console geometry the ejected film is continuous in the span-wise direction (in contrast to cylindrical holes), and the film will not lift off from the blade surface when increasing the blowing ratio. Consequently, the region in vicinity of the slot injection is highly protected from hot gases and laterally averaged effectiveness can reach the maximum value of unity as it is in the computational results. The kidney shape phenomenon in the region of adjacent consoles which is observed in the experimental work of Sargison et al., and captured in the present investigation, is shown in Fig. 7, a. To highlight what happens in this region, secondary flow velocity vectors and the corresponding temperature contours are plotted at positions immediately behind the injection ($x/d = 5$) and far downstream ($x/d = 20$).

Fig. 7, a and b shows the results for cylindrical hole injection, Fig. 7, c and d represents the console geometry. Due to the lack of space, only the middle momentum ratio is represented here ($I = 0.48$ for the cylinder and $I = 0.36$ for the console). At $x/d = 5$, near the injection

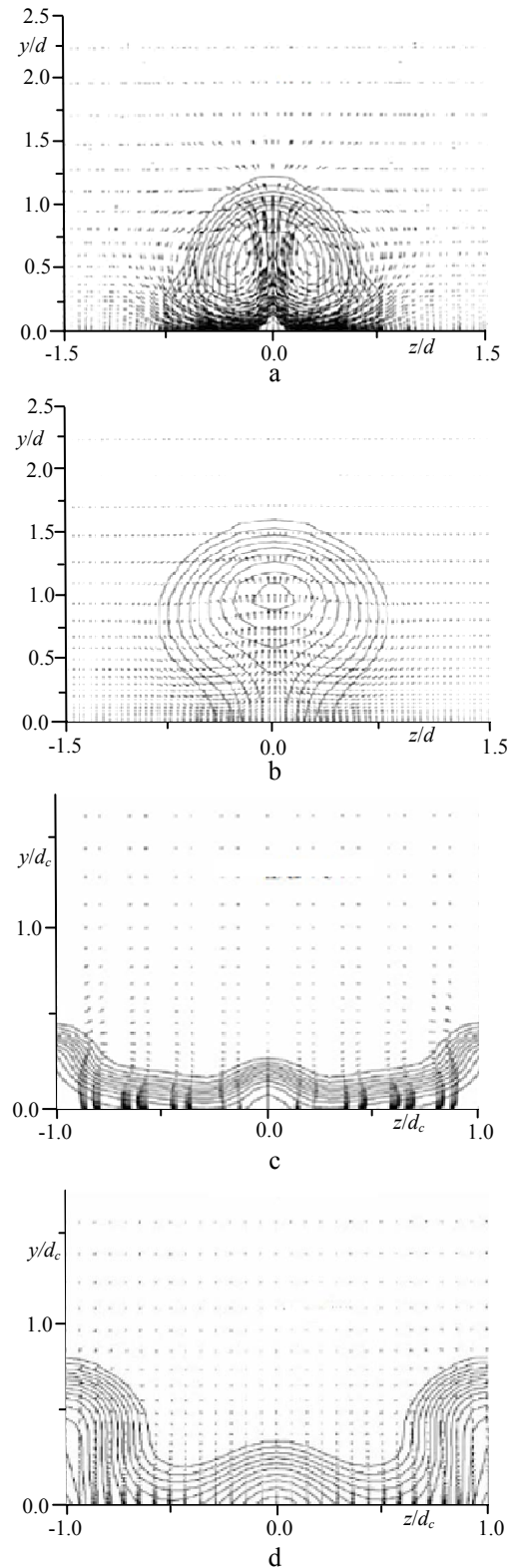


Fig. 7 Secondary flow velocity vectors and temperature contours: a - cylinder, $I = 0.36$ and $x/d = 20$; b - cylinder; $I = 0.48$ and $x/d = 20$; c - console, $I = 0.36$ and $x/d = 5$; d - console, $I = 0.36$ and $x/d = 20$

hole, the cylindrical case shows the well known structure of kidney shape characterized by the two contra rotating vortices. Further downstream ($x/d = 20$), the two contra rotation vortices are still there but less strong and having their center far from the wall, flag Fig. 7, a and b. These

vortices disappear in the console geometry, Fig. 7, c and d. However, due to the divergence in the console passage, laterally injected flow is observed. Interaction between two adjacent consoles leads to another kind of the contra rotating vortices but much more lower than those of the cylindrical injection.

6. Conclusion

Numerical investigation of three holes geometries for film cooling is done with the help of the well stabilized CFX code from ANSYS Inc. The SST turbulence model coupled with automatic wall strategy is applied with success to highlight the main features of the thermal fluid flow of such a complex configuration. The main conclusion is that the new console film-cooling geometry presents a very promising improvement in thermal performance. Increasing the blowing ratio does not lead to deterioration of thermal protection as it is the case with discrete hole injection. Further numerical and experimental studies are required to verify the mechanical strength of the blade supplied with such film cooling consoles and it probably is more than the rectangular slot. If satisfied, the new geometry will be a very promising way to improve the gas turbine blade cooling strategies.

Acknowledgements

This work was supported by the laboratory of the applied mechanics of the University of Sciences and Technologies of Oran-Algeria with the assistant of professor Azzi. A.

References

1. **Goldstein, R.J.** Advances in Heat Transfer.-Academic Press. -NewYork, 1971, p.321-379.
2. **Bergles, G., Gosman, A.D. & Launder, B.E.** The near-field character of a jet discharged normal to a main stream. -Trans. ASME C: J. Heat Transfer, 1976, 98, p.373-378.
3. **Andreopoulos, J., Rodi, W.** Experimental investigation of jets in a crossflow. -Journal of Fluid Mechanics, 1984, 138, p.93-127.
4. **Sargison, J.E., Guo, S.M., Oldfield, M.L., Lock, G.D., Rawlinson, A.J.** A converging slot-hole film-cooling geometry-part 1: low-speed flat-plate heat transfer and loss. -ASME J. Turbomachinery, 2002, 124, p.453-460.
5. **Abbès AZZI & Bassam, Jubran, A.** Numerical modeling of film cooling from converging slot-hole. -Heat Mass Transfer, 2006, 43, p.381-388.
6. **Menter, F.R.** Zonal two-equation ω - k turbulence model for aerodynamic flows.-AIAA, 1993, p.93-2906.
7. **Kandula, M., Wilcox, D.C.** An examination of k - ω Turbulence Model for Boundary Layers, Free Shear Layers, and Separation Flows, AIAA 1995 Paper, 95-2317.
8. **Jones, W.P., Launder, B.E.** The prediction of laminarization with a two-equation model of turbulence. -International Journal of Heat and Mass Transfer, 1972, 15, p.301-14.
9. **Margason, R.J.** Fifty Years of Jet in Cross-Flow Research. -AGARDCP-534, 1993, p.1.1-1.41.
10. **Šinkūnas, S., Kiela, A.** On momentum transfer in a falling turbulent liquid film. -Mechanika. -Kaunas: Technologija, 2008, Nr.2(70), p.22-26.
11. **Šinkūnas, S., Kiela, A.** Effect of the temperature gradient on heat transfer and friction in laminar liquid film. -Mechanika. -Kaunas: Technologija, 2009, Nr.1(75), p.31-35.

A. Khorsi, A. Azzi

TRIJŲ SKIRTINGOS GEOMETRIJOS KIAURYMIŲ AUŠINIMO PLĖVELĖS SKAIČIAVIMAS

R e z i u m ė

Straipsnyje pateikiami trijų kiaurymių aušinimo plėvelių geometrijos skaičiavimai. Pirmoji yra klasikinė cilindrinė kiaurymė, antroji keturkampė, o trečioji – nauja siaurėjanti, suprojektuota norint pagerinti aušinimo kanalo geometriją, kad atskirose kiaurymėse sumažėtų mechaninė jėga. Tiksliai Sargisono ir kitų (2002) sukurta eksperimentinė geometrija yra naudojama taikant ANSYS ICEM CFD programą. Palyginimui išbandyti trys pūtimo greičiai. Skaičiuojamoji aplinka yra diskretizuota naudojant patobulintą daugiablokį konstrukcinį tinklėlį, o slėgio (pūtimo) plotas ir turbulencijos laukas nustatyti naudojant Menterio (1983) ribinių tangentinių įtempių modelį. Pateikti ir palyginti pasvirusių cilindrinėse kiaurymių skaičiavimo, esant įvairiems pūtimo greičiams, rezultatai, kanalai ir nauja geometrija. Tyrimas parodė, kad kiaurymių išėjimą geriau yra jungti išpjovų forma. Tada aušimo plėvelė nenutrūkstamai teka pūtimo kryptimi ir jos srovė, esant dideliems pūtimo greičiams, nedidėja.

A. Khorsi, A. Azzi

COMPUTATION FILM COOLING FROM THREE DIFFERENT HOLES GEOMETRIES

S u m m a r y

The paper presents computations of three film cooling geometries. The first one is the classical cylindrical hole, the second represents a rectangular slot and the third one is a new converging slot hole (CONSOLE) who is designed to offer an improved cooling of slot geometry, while retaining the mechanical strength of discrete holes. The exact experimental geometries of Sargison et al. (2002) are reproduced using the ANSYS ICEM CFD software. For comparison purpose three values of the blowing ratio are tested. The computational domain is discretized using a refined multi-bloc structured grid including the plenum area and the turbulence field is resolved by using the SST Model of Menter (1993). Computational results of inclined cylindrical holes, slot and the new geometry are presented and compared for different blowing ratios. The investigation indicates that joining the hole exits in a slot form has the advantages of keeping the ejected coolant film continuous in the span-wise direction, and delaying the coolant-jet lift-off occurring at relatively high blowing ratios.

А. Кхорзи, А. Аззи

РАСЧЕТ ОХЛАЖДАЮЩЕЙ ПЛЕНКИ ДЛЯ ТРЕХ ОТВЕРСТИЙ РАЗЛИЧНОЙ ГЕОМЕТРИИ

Резюме

Статья представляет расчет геометрии охлаждающих пленок для трех отверстий. Первая это классическое цилиндрическое отверстие, вторая – представляет собой канал четырехугольного сечения и третья – новое сужающееся отверстие, которое спроектировано для улучшения геометрии канала, с целью уменьшения механической силы в отдельных отверстиях. Точная экспериментальная геометрия Саргисона и других (2002) использована при применении ANSYS ICEM CFD программы. Для сравнения использованы три скорости продувки. Расчетное пространство дис-

кретизовано при помощи модифицированной многоблочной конструкторской сетки, оценивая площадь продувки, а поле турбуленции определено используя модель предельных тангенциальных напряжений Менгера (1983). Результаты расчета наклонных цилиндрических отверстий, каналы и их новая геометрия представлена и проверена для разных скоростей продувки. Исследование показало, что соединение выхода отверстий при помощи вырезов является более предпочтительным для поддержания непрерывности охлаждающей пленки в направлении продувки и уменьшения скорости охладителя при больших скоростях продувки.

Received June 15, 2010

Accepted December 07, 2010

DOI: 10.5755/j02.mech.15971